Design of the Ball Screw Mechanism for Optimal Efficiency

M. C. Lin

S. A. Velinsky

B. Ravani

Department of Mechanical & Aeronautical Engineering, University of California—Davis, Davis, CA 95616

This paper develops theories for evaluating the efficiency of the ball screw mechanism and additionally, for designing this mechanism. Initially, a quasi-static analysis, which is similar to that of the early work in this area, is employed to evaluate efficiency. Dynamic forces, which are neglected by the quasi-static analysis, will have an effect on efficiency. Thus, an exact theory based on the simultaneous solution of both the Newton-Euler equations of motion and the relevant kinematic equations is employed to determine mechanism efficiency, as well as the steady-state motion of all components within the ball screw. However, the development of design methods based on this exact theory is difficult due to the extensive computation necessary and thus, an approximate closed-form representation, that still accounts for the ball screw dynamics, is derived. The validity of this closed-form solution is proven and it is then used in developing an optimum design methodology for the ball screw mechanism based on efficiency. Additionally, the self-braking condition is examined, as are load capacity considerations.

Introduction

The ball screw mechanism (BSM) has been used for many years in a wide variety of applications. The most referred to work on the BSM is due to Levit (1963a, 1963b). In his work, Levit has both reviewed the literature prior to his, as well as providing a series of calculations for designing this mechanism. Levit's work has provided the foundation for most of the subsequent work on the design and manufacture of this mechanism including that of Belyaev and associates (1971, 1973, 1974a, 1974b, 1981, 1983), Drozdov (1984) and Mukhortov (1982), to name a few. Unfortunately, Levit includes several improper assumptions causing his results, as well as those based on his results, to be questionable. These errors are noted by Lin et al. (1994), who have taken a fundamental approach in examining the kinematics of the BSM. Basically, Levit does not account for the torsion of the helical path of the individual ball center.

In this paper, we will first examine the efficiency of the BSM using a quasi-static approach much like Levit's, but with the proper kinematics. Since dynamic forces are neglected by the quasi-static analysis, a more exact approach will be taken. In this approach, we will consider the steady-state motion of the ball for a three-point-contact profile (Gothic profile) without deformation by numerically solving the Newton-Euler equations and the relevant kinematic equations simultaneously. While the efficiency of the BSM actually varies as a function of time, the steady-state simplification is valid for many applications and additionally, it can be more easily applied for developing design methods. Closed-form solutions are even more easily applied to the development of design methods and such solutions are derived in this paper. These closed-form solutions, which account for the dynamic forces, are shown to be valid through close agreement with the results of the steady-state theory. A detailed design methodology for the BSM based on the closed-form theory is then presented.

In general, the analysis of the ball screw motion can be divided into two different categories according to the driving component; i.e., nut driving or screw driving. Additionally, each of these categories can be further divided according to the type of input motion; i.e., conversion of rotary into linear motion or conversion of linear into rotary motion. Since the procedures for analyzing the different types of motion are similar and all types of motion are kinematic inversions of each other, in this paper, we will only examine the cases with the screw as the driving component.

Quasi-Static Efficiency Analysis

Levit, in his classic work on the BSM, assumes that there is no-slip between the balls and the nut and screw. Thus, he derives the quasi-static ball screw efficiency by assuming that there is only rolling resistance at the ball/screw and ball/nut contact points. Levit's results imply that the upper bound on ball screw efficiency should be unity. However, recent detailed examination of the kinematics of the BSM proves that the no-slip condition is not attainable and that there must be slip on the normal plane of at least one contact point; see Lin et al. (1994). Therefore, in this work, we have used the correct kinematics and have assumed both slip on the normal plane and rolling resistance in the tangent direction at the contact points in order to determine the quasi-static efficiency of the BSM. Additionally, we assume that there are two contact points between an individual ball and the screw and nut.

For the case of screw driving, suppose that a moment, Mk, is acting on the screw in order to overcome an axial load $F_a\mathbf{k}$

Contributed by the Mechanisms Committee for publication in the JOURNAL OF MECHANICAL DESIGN. Manuscript received March 1990; revised Feb. 1994. Associate Technical Editor: G. L. Kinzel.

applied on the nut. By considering static equilibrium of the screw, the ball and the nut, respectively, we arrive at the following relations:

$$M = r_m Q_n \{ S_\alpha C_\rho [S_\beta + f(a - C_\beta)] + C_\alpha S_\rho \},$$

$$Q_A \approx Q_B \equiv Q_n, \text{ and}$$

$$F_a = -Q_n [C_\alpha C_\rho (S_\beta - f C_\beta) - S_\alpha S_\rho] \quad (1)$$

where

M = the torque applied on the screw or the nut,
F_a = the axial force applied on the screw or the nut,
Q_i = the normal force at the contact points between the ball and nut and screw, respectively, and the corresponding subscripts: A and B denote the points between the ball and the nut and between the ball and the screw, respectively,
f = the Coulomb coefficient of friction at the contact points,
r_m = mean radius of the helical path of the ball centerline,
r_b = ball radius,
a = r_b/r_m,
α = helix angle of the path of the ball centerline,
C_i, S_i = cosine and sine functions, respectively, with the angle denoted by the subscript, and we will later use
t_i = tangent function with the angle denoted by the subscript.

The friction angle, ρ, is used to represent the dissipated energy due to rolling friction between the contact surfaces and can be represented by the following expression, which was derived by Levit:

$$\rho = \tan^{-1}\left[\frac{f_r}{r_b S_\beta}\right] \quad (2)$$

where f_r denotes the rolling coefficient of friction. We additionally assume that the contact angles between the ball and the screw and nut, β_A and β_B, respectively, are equal; i.e., $\beta_A = \beta_B = \beta$.

The efficiency is equal to the ratio of the work done by the output forces to the work done by the input and can be represented as

$$\eta = 1 - \frac{fa + t_\rho/(C_\alpha S_\alpha)}{S_\beta + f(a - C_\beta) + t_\rho/t_\alpha}. \quad (3)$$

Using a similar approach for the case of nut driving, the efficiency can be simply expressed as

$$\eta = 1 - \frac{f(a + 2C_\beta) + t_\rho/(C_\alpha S_\alpha)}{S_\beta + f(a + C_\beta) + t_\rho/t_\alpha}. \quad (4)$$

A More Exact Efficiency Analysis

The quasi-static analysis of the preceding section provides an approximation to the ball screw's efficiency since dynamic forces, which will have an effect, have been neglected. In actuality, ball screw efficiency will vary as a function of time due to the system dynamics and the time-dependent nature of the input torque. In order to design with utmost care, one would need to solve the general equations of motion in order to calculate the time varying efficiency, and corresponding design methods could be developed that consider either a maximum or a mean value of efficiency. However, such an approach would be quite tedious and results may be difficult to use for design purposes. By considering steady-state ball screw motion, an approximation of the equations of motion is obtained that still accounts for some of the dynamic forces. This approximation provides a basis for developing a simplified design method and it is valid for many ball screw applications. Since the steady-state theory results in an approximate efficiency, in certain instances, the designer may elect to integrate the general equations of motion in order to monitor the time varying efficiency.

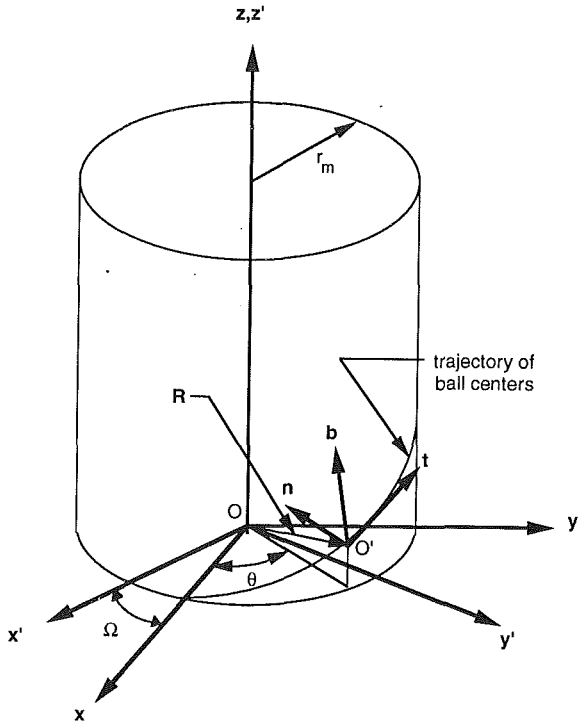

Fig. 1 The position of the ball center, O′, in Cartesian coordinates and Frenet-Serret coordinates

To develop the equations of motion, we first consider the position of the ball center and we employ the following three coordinate frames: a fixed Cartesian frame, $ox'y'z'$, a Cartesian frame rotating with the screw, $oxyz$, and a Frenet-Serret coordinate frame along the ball trajectory, $o'nbt$, as shown in Fig. 1. We then arrive at the Newton-Euler equations which represent the ball motion. The steady-state form of these equations of motion, for the case of converting rotary into linear motion, follow.

$$f(Q_B S_{\psi B} + Q_A S_{\psi A} + Q_{A'} S_{\psi A'}) = 0 \quad (5a)$$

$$Q_A(C_\beta - f S_\beta C_{\psi A}) - Q_B(C_\beta + f S_\beta C_{\psi B}) + Q_{A'}(C_\beta + f S_\beta C_{\psi A'}) = m r_m (\dot\theta + \dot\Omega)^2 \quad (5b)$$

$$Q_A(S_\beta + f C_\beta C_{\psi A}) - Q_B(S_\beta - f C_\beta C_{\psi B}) - Q_{A'}(S_\beta - f C_\beta C_{\psi A'}) = 0 \quad (5c)$$

$$f r_b (Q_B C_{\psi B} - Q_A C_{\psi A} - Q_{A'} C_{\psi A'}) = -I(\dot\theta + \dot\Omega)\omega_n C_\alpha \quad (5d)$$

$$f r_b S_\beta (Q_B S_{\psi B} - Q_A S_{\psi A} + Q_{A'} S_{\psi A'}) = I(\dot\theta + \dot\Omega)(\omega_t C_\alpha - \omega_b S_\alpha) \quad (5e)$$

$$-f r_b C_\beta (Q_B S_{\psi B} - Q_A S_{\psi A} - Q_{A'} S_{\psi A'}) = I(\dot\theta + \dot\Omega)\omega_n S_\alpha \quad (5f)$$

where:

ψ_i = the angle between the direction of the friction force and the normal plane at the contact points, and the corresponding subscripts: A and A' denote the major and minor contact point between the ball and the nut, respectively, and B denotes the major contact point between the ball and the screw,
m = mass of an individual ball,
I = mass moment of inertia of the ball relative to its mass center,
$\dot\theta$ = the angular velocity of the ball relative to the screw along the helical path,

$\dot{\Omega}$ = the angular velocity of the screw, and
$\omega_n, \omega_t, \omega_b$ = the angular velocity of the ball with respect to its center of mass in the normal, tangential and binormal directions of the helical path.

Note that these equations assume a three-point contact profile between the ball and the nut and screw. With the three-point contact, there are two major contact points, A and B, through which the majority of the load is transferred. Additionally, a minor contact point, A', must exist in order to equilibrate the centripetal force and adequately constrain the ball. We additionally assume that the contact angles between the ball and the screw and nut, β_A, $\beta_{A'}$, and β_B, respectively, in this case, are equal; i.e., $\beta_A = \beta_{A'} = \beta_B = \beta$. From a design perspective, equal contact angles result in consistent loading over all of the contact points helping prevent local failure and premature fatigue. Theoretically, the contact angle can be between 0 deg. and 90 deg. In actuality, the contact angle is limited by geometry and manufacturing techniques and is most often between 45 deg. and 60 deg. The interested reader is again referred to Lin et al. (1994) for a more detailed derivation of these equations, as well as those to follow.

The slip angles, the angles between the friction force directions and the normal plane at the contact points, are better defined as

$$\psi_i = \pi + \tan^{-1}\left(\frac{V_{yi}}{V_{xi}}\right) \tag{6}$$

where V_{xi} and V_{yi} denote the magnitude of the velocity in the normal plane and the tangential direction, respectively, with respect to the local coordinate systems at the contact points; see Fig. 2. Through a study of the kinematics (see Lin et al., 1994), the following slip velocities result:

For the ball/nut contact point:

$$V_{xA} = -r_b\omega_t \text{ and } V_{yA} = d(\dot{\theta}+\dot{\Omega}) + r_b(\omega_b C_\beta - \omega_n S_\beta) \tag{7}$$

and for the ball/screw contact point:

$$V_{xB} = r_b(\omega_t - \dot{\Omega}S_\alpha) \text{ and}$$

$$V_{yB} = d\dot{\theta} - r_b[(\omega_b - \dot{\Omega}C_\alpha)C_\beta - \omega_n S_\beta] \tag{8}$$

where $d = r_m/C_\alpha$.

By imposing static equilibrium on the screw and nut, we have the following expressions which can be used to relate the torque applied to the screw (or nut) to the axial load acting on the nut (or screw):

$$M = ({}^r\mathbf{R}_i \times \mathbf{F}_i + {}^r\mathbf{R}_{i'} \times \mathbf{F}_{i'})\cdot\mathbf{k}$$
$$= r_m\{w_l(Q_{i'} - Q_i)S_\alpha S_\beta + f[-S_\alpha(Q_i C_{\psi i} + Q_{i'}C_{\psi i'})(w_l a + C_\beta)$$
$$+ C_\alpha(Q_i S_{\psi i} + Q_{i'}S_{\psi i'})(1 + w_l a C_\beta)]\} \text{ and}$$

$$F_a = (\mathbf{F}_i + \mathbf{F}_{i'})\cdot\mathbf{k}$$
$$= w_l(Q_i - Q_{i'})C_\alpha S_\beta + f[C_\alpha C_\beta(Q_i C_{\psi i} + Q_{i'}C_{\psi i'})$$
$$+ S_\alpha(Q_i S_{\psi i} + Q_{i'}S_{\psi i'})]; \quad i = A, B. \tag{9}$$

where

${}^r\mathbf{R}_i$ = the position vector of contact point i with respect to the rotational Cartesian coordinate system (see Fig. 1),
$\mathbf{F}_i$ = the force vector applied on the ball at contact point i, and

the weighting function, w_l, allows distinction between the various contact points and is defined as

$w_l = 1$ for $i = A$ (A denotes the ball/nut contact)

$= -1$ for $i = B$ (B denotes the ball/screw contact).

Equation (9) provides two simultaneous equations for either the screw driving or the nut driving case. When a torque is applied to the nut, the subscript $i = A$ will apply for the moment equation and the subscript $i = B$ will apply for the force equation since an axial force will be acting on the screw. When the torque is applied to the screw, $i = B$ applies for the moment equation and $i = A$ applies for the force equation.

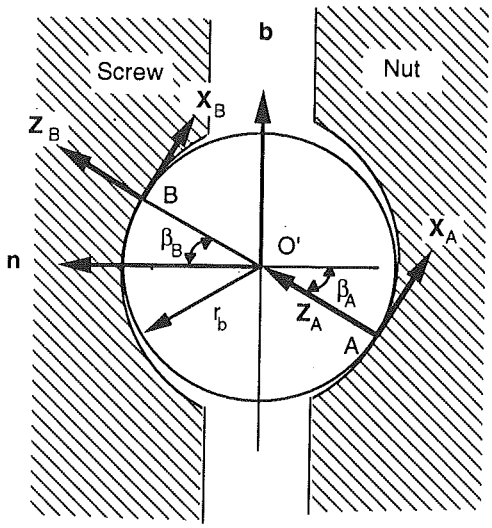

Fig. 2 Coordinate systems at the contact points

Equations (5)–(9) have been solved numerically for the screw driving case with the following ball screw parameter values: r_b = 4.37 mm (0.172 in.), r_m = 24.3 mm (0.956 in.), Ω = 2000 rpm, and α = 10 deg. for varying contact angles or β = 45 deg. for varying helix angles. The coefficient of friction, f, is assumed equal to 0.075, a value representative of the contact conditions normally found in the BSM and this value will be used for the remainder of the paper. Additionally, it is assumed that an axial load, F_a, equal to 2113 Nt (475 lb) is resisting motion of the nut. Figures 3 and 4 depict the results. We show the relationships between efficiency and contact angle and helix angle in Fig. 3. Figure 4 displays the normal loads as a function of contact angle. In this figure, the curve represents the load at the major contact points, A and B, which, for all practical purposes, are equal, and the load at the minor contact point, A', which is orders of magnitude smaller, is not distinguishable from the abscissa.

The Approximate Closed-Form Solution

The theory developed above involves the numerical solution of the set of equations representing the steady-state motion of the ball screw and designing ball screw mechanisms using this theory is obviously quite cumbersome. The current section derives an approximate closed-form solution for the ball screw motion and considerable insight is gained into the sensitive design parameters. This solution also allows us to investigate the optimal design of the BSM.

For the mechanism operating at relatively low speed, which is true for most BSM currently used in industry, it is reasonable to assume that the centripetal force is very small compared with the normal loads. Additionally, from the numerical results above, we recognize that the normal load at the minor contact point is very small compared to the normal loads at the two major contact points. The third contact point is necessary to provide a stable system, but has only little effect on the resultant motion at these relatively low speeds. Thus, $Q_A \approx Q_B$, indicating that a two-point-contact model is a reasonable approximation. For the particular size of balls used in this model, we find that this approximation is valid for screw speeds as high as 2,000 rpm.

With the assumption that $Q_{A'} = 0$, from Eq. (5a), we obtain

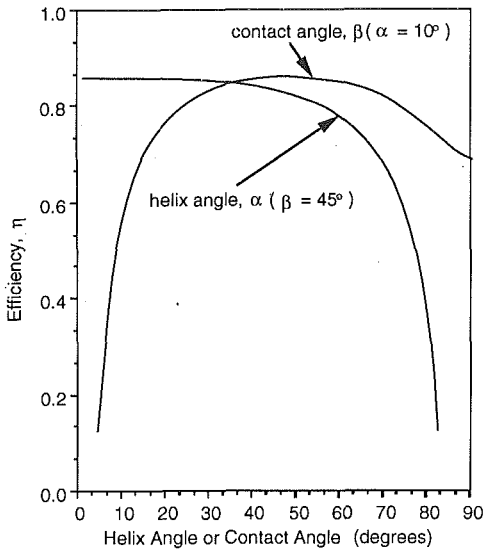

Fig. 3 Efficiency as a function of helix angle or contact angle—conversion of rotary into linear motion

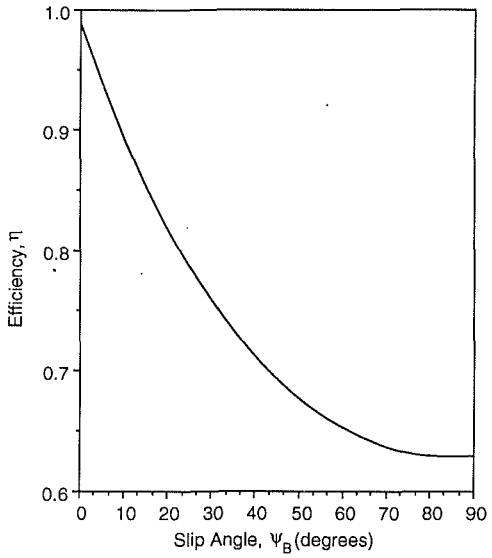

Fig. 5 Efficiency as a function of the slip angle between the ball and the screw

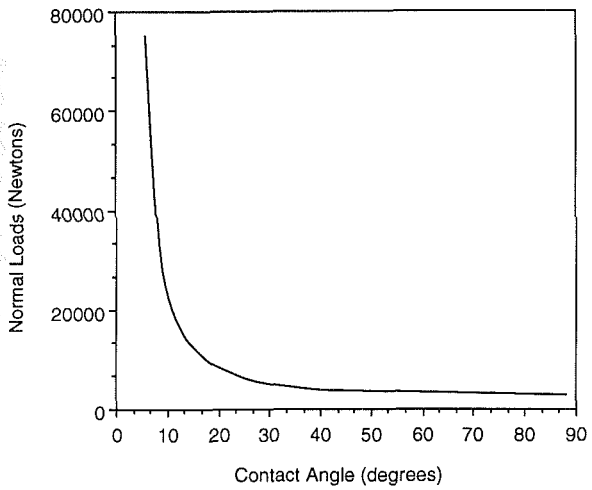

Fig. 4 Normal loads as a function of contact angle—conversion of rotary into linear motion, screw driving

$$\frac{Q_A}{Q_B} = -\frac{S_{\psi B}}{S_{\psi A}} \cong 1 \tag{10}$$

which implies that $\psi_A \approx \pi + \psi_B$. Note that this result also agrees well with the numerical results.

We note that the nut moves a distance equal to $-\Omega L/2\pi = -\Omega r_m t_\alpha$ (where L denotes the lead of the screw) as the screw rotates through an angle Ω. Thus, from the above assumptions and Eq. (9), the efficiency of the BSM, η, can now be written in closed-form as

$$\eta = \frac{S_\beta - f(C_\beta C_{\psi A} + S_{\psi A} t_\alpha)}{S_\beta + f[C_{\psi B}(a - C_\beta) + S_{\psi B}(1 - aC_\beta)/t_\alpha]}. \tag{11}$$

It is now simple to observe the effects of the various parameters on efficiency.

Figure 5 shows the variation in efficiency with respect to the slip angle at the screw/ball contact point, ψ_B. In this figure, the following parameter values are used: $a = 0.1$ and $\alpha = 10$ deg. The curve indicates that the friction along the tangential direction dissipates more energy than that on the normal plane. In other words, the component of frictional force along the tangential direction plays a more important role, from the efficiency point of view, than that on the normal plane. Thus, the upper and lower limits of efficiency are at $\psi_B = 0$ deg. (normal plane) and $\psi_B = 90$ deg. (tangential direction), respectively. We note that we could arrive at the same conclusions by using the slip angle at the screw/ball contact point, ψ_A, since $\psi_A \approx \pi + \psi_B$.

Furthermore, the following equation is obtained by dividing Eq. (5*f*) by Eq. (5*d*):

$$\cot(\psi_A) + \cot(\psi_B) = \frac{2C_\beta}{t_\alpha}. \tag{12}$$

By combining Eqs. (10) and (12), we have

$$\psi_B = \psi_A - \pi = \tan^{-1}\left(\frac{t_\alpha}{C_\beta}\right). \tag{13}$$

Therefore, Eq. (11) can be further simplified to

$$\eta = 1 - \frac{f}{C_\alpha^2 S_\beta\left[\sqrt{C_\beta^2 + t_\alpha^2} + fS_\beta\right]} \tag{14}$$

and we note that the only parameters affecting efficiency from this equation are the coefficient of friction, the helix angle and the contact angle.

Using Eq. (14), we find that the efficiencies generated are nearly identical to the numerical results obtained from the steady-state solution of the Newton-Euler equations shown in Fig. 3 where the maximum difference between the theories for the efficiency versus helix angle relationship is 0.33 percent and between the theories for the efficiency versus contact angle relationship is 0.86 percent. Thus, Eq. (14) is a valid representation of the efficiency of the BSM for this type of motion. Further investigation of Fig. 3 reveals that an optimum contact angle exists for peak efficiency. This existence of an optimum can be explained as follows. If one considers only the friction on the normal plane, the efficiency is proportional to the contact angle, which can be observed through Eq. (11). However, from Fig. 5, the component of frictional force along the tangential direction, which dissipates more energy than that on the normal plane, becomes more important at higher contact angles. Hence, a peak efficiency exists at a contact angle at which the two frictional components reach some particular ratio. To obtain the optimum contact angle mathematically, we differentiate the denominator of Eq. (14) with respect to

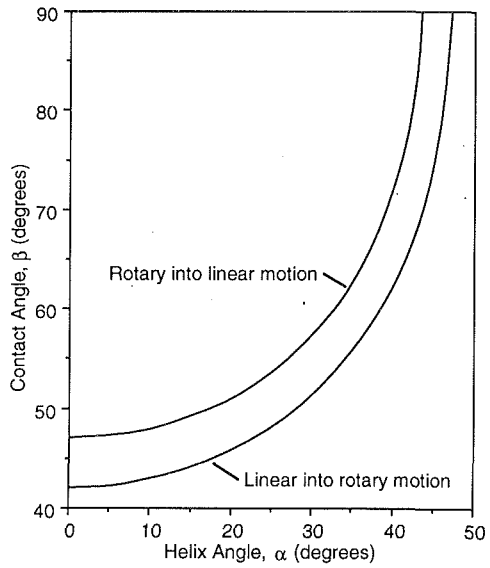

Fig. 6 Relationship between contact angle and helix angle to achieve optimal efficiency

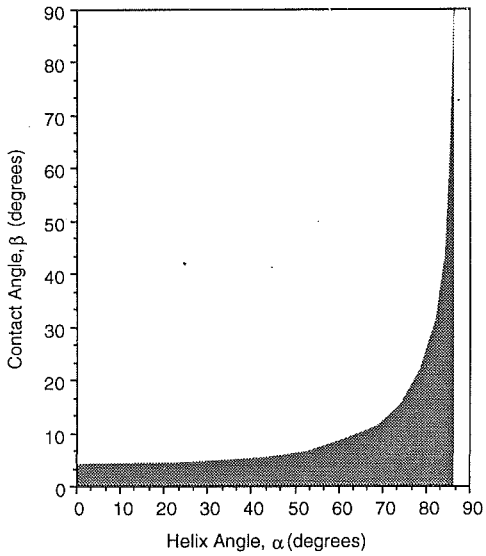

Fig. 7(*a*) The self-braking design space—conversion of rotary into linear motion

the contact angle and set the derivative equal to zero, resulting in the following expression.

$$C_\beta^2 + t_\alpha^2 + 2fS_\beta\sqrt{C_\beta^2 + t_\alpha^2} = S_\beta^2 \tag{15}$$

One notes, from this equation, that the optimum contact angle can be expressed as a function of helix angle. The resultant relationship is depicted in Fig. 6. This curve indicates that the peak efficiency exists only at lower helix angles and higher contact angles. The optimum efficiency is arrived at by merely solving Eqs. (14) and (15) simultaneously. The resulting optimal efficiency value is 86.1 percent for all helix angles and the corresponding contact angle from Eq. (15), and the coefficient of friction equal to 0.075.

Self-braking is that condition in which it is kinematically impossible for the mechanism to perform useful work and is, of course, highly undesirable. The self-braking condition is determined by combining Eqs. (11) and (13) and results when the numerator of Eq. (11) becomes negative; i.e.,

$$S_\beta \le f\sqrt{C_\beta^2 + t_\alpha^2}. \tag{16}$$

The shaded region below the curve in Fig. 7a represents the design space in which self-braking occurs. We note that self-braking takes place for designs with low contact angles for the helix angles normally used and additionally, that the self-braking condition always takes place at the driven side of the mechanism.

Conversion of Linear into Rotary Motion. Employing a similar procedure as above, we obtain the efficiency for the case of converting linear into rotary motion as

$$\eta = 1 - \frac{f}{C_\alpha^2\left[S_\beta\sqrt{C_\beta^2 + t_\alpha^2} + f(C_\beta^2 + t_\alpha^2)\right]}. \tag{17}$$

It is again easy to develop relationships between efficiency and contact angle and helix angle. For this case, the trends are the same as the case of converting rotary into linear motion, but with slightly different values. Now, the peak efficiency occurs when the following expression holds:

$$C_\beta^2 + t_\alpha^2 = S_\beta^2 + 2fS_\beta \tag{18}$$

and the resulting relationship between contact angle and helix angle is additionally shown in Fig. 6. This curve also indicates that the peak efficiency exists only at lower helix angles and higher contact angles. The optimum efficiency is arrived at by merely solving Eqs. (17) and (18) simultaneously. As in the case of conversion of rotary to linear motion, the optimal efficiency value is 86.1 percent for all helix angles and the corresponding contact angle from Eq. (18), and the coefficient of friction equal to 0.075. In this case, the self-braking condition occurs when

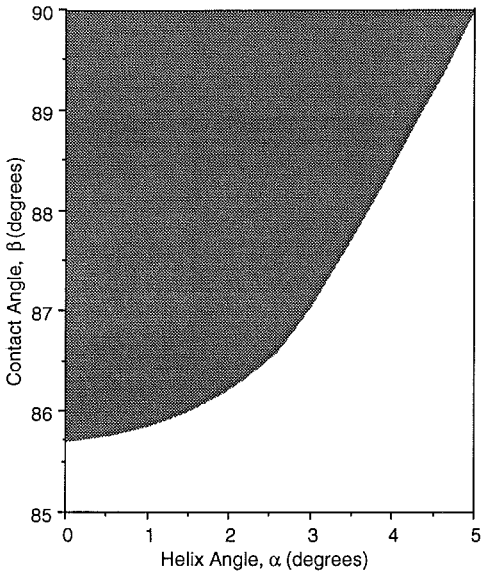

Fig. 7(*b*) The self-braking design space—conversion of linear into rotary motion

$$fS_\beta \ge \sqrt{C_\beta^2 + t_\alpha^2}. \tag{19}$$

The shaded region above the curve in Fig. 7(*b*) depicts the design space for self-braking and this takes place only for designs with low helix angles and high contact angles.

Load Capacity Considerations

The normal load transmitted through the contact surfaces should be designed to be as low as possible for a given loading

condition to attain the highest possible load capacity. For the case of conversion of rotary into linear motion, we consider a constant load F_a. Then, by neglecting the friction force terms which result in surface tractions as opposed to normal loads, from Eq. (9), we notice that causing $C_\alpha S_\beta$ to be as high as possible results in the lowest normal loads. This implies that designs with small helix angles and large contact angles give the BSM the maximum load capacity. With the ball-screw designed such that it operates at its maximum efficiency, we find that the term $C_\alpha S_\beta$ is constant for all helix angles and the corresponding contact angle from Eq. (15), and thus, the load carrying capacity cannot be improved for this optimum case.

For the case of conversion of linear into rotary motion, assuming constant load M, Eq. (9) reveals that the lowest normal loads occur for a high $r_m S_\alpha S_\beta$ term. This indicates that with large mean radius, helix angle and contact angle, the BSM has the highest load capacity. Additionally, we note that the parameter a (ratio of ball radius to mean radius) is not a critical parameter within the range found in most industry applications; i.e., usually, $0.07 \leq a \leq 0.2$. Thus, for this case, one would like to choose the highest contact angle that is possible given manufacturing constraints and select the corresponding helix angle from Eq. (18) for optimum efficiency in order to design the most efficient, highest load carrying ball screw mechanism.

Design Procedure

Based on the results arrived at in the preceding analysis, the following methodology is recommended for the design of the BSM:

(*1*) Select a preliminary helix angle based on the discussion related to load capacity and the corresponding motion.

(*2*) Determine the contact angle for optimal efficiency from either Eq. (15) or (18).

(*3*) Choose the screw length according to the application requirements.

(*4*) Determine the mean radius such that $r_m \geq$ screw length/60, as noted by Levit (1963b).

(*5*) Select the ball size such that $0.07 \leq a \leq 0.2$.

(*6*) Determine the thread profiles such that $0.95 \leq r_b/r_2 \leq 0.97$, where r_2 = the radius of curvature of the thread profile for the nut or screw.

(*7*) Determine the approximate contact force from the specified resistive force or moment and the equations shown below, which were derived from Eq. (9) with friction neglected.

For the conversion of rotary into linear motion:

$$Q_i = \frac{F_a}{C_\alpha S_\beta} \tag{20}$$

For the conversion of linear into rotary motion:

$$Q_i = \frac{M}{r_m S_\alpha S_\beta} \tag{21}$$

(*8*) Determine the relative motion between the screw and the nut from the following relationship:

$$\text{advance distance} = (r_m t_\alpha)\ \text{(angular displacement)}.$$

(*9*) Calculate the maximum contact stress using the approximate contact load, the ball radius, the thread radius of curvature and Hertz' theory.

(*10*) Determine the efficiency of the BSM from Eqs. (14) or (17).

This procedure should be an iterative process with a new set of ball screw dimensions selected if any of the criteria are violated. For instance, if the contact stresses determined from the Hertzian theory are too high, most likely larger dimensions are necessary. Similarly, if the relative motion is not appropriate (size constraints are violated), a new helix angle, as well as other dimensions, may be necessary. Additionally, this procedure has not discussed the speed requirements nor the available motor power of the application. Obviously, these factors will also affect the final design.

Conclusions

This paper provides a powerful set of tools for analyzing and designing the ball screw mechanism. The exact steady-state motion within the ball screw mechanism has been determined by numerically solving the Newton-Euler equations of motion and the kinematic equations simultaneously. This paper has developed a simplified closed-form solution for ball screw motion and has employed this theory in considering the optimum design of this mechanism. In terms of efficiency, the driving component does not have an effect. That is, only the type of motion conversion is important. Thus, the necessary relationship between contact angle and helix angle for optimum efficiency has been formulated for all types of ball screw motion. Additionally, the conditions for self-braking have been discussed as well as the load capacity of the BSM. The results of the closed-form solution have been presented in a dimensionless manner allowing this work to be applied to the design of any ball screw mechanism. Finally, a complete design procedure for the BSM has been developed.

Acknowledgment

This research was supported in part by US Army Research Office grant number DAAL03-90-G-005 and the California Department of Transportation through the AHMCT program.

References

Belyaev, V. G., 1971, "Re-entry of Balls in Recirculating Ball-screw-and-nut Mechanisms," *Russian Engineering Journal*, Vol. LI, No. 11, pp. 30–34.

Belyaev, V. G., and Kogan, A. I., 1973, "Effect of Geometrical Errors of Ball Contact Angle in Ball-Screw Transmissions," *Machines & Tooling*, No. 5, pp. 25–29.

Belyaev, V. G., and Drobashevskii, G. S., 1974a, "Recirculating Ball Nut and Screw Transmissions with Arched and Semi-circular Thread Profiles," *Russian Engineering Journal*, Vol. LIV, No. 9, pp. 18–21.

Belyaev, V. G., and Kogan, A. I., 1974b, "Effect of Screw Diameter Variations on Accuracy and Stiffness of Recirculating Ball Nut-Screw Pairs," *Machines & Tooling*, Vol. XLV, No. 9, pp. 16–18.

Belyaev, V. G., and Turavinov, V. P., 1981, "Positioning Accuracy of Ball-Screw Mechanism," *Soviet Engineering Research*, Vol. 1, No. 5, pp. 34–36.

Belyaev, V. G., and Malyuga, V. S., 1983, "The Force Transfer Factor in the Return Channel of a Ball and Screw Mechanism," *Soviet Engineering Research*, Vol. 3, No. 2, pp. 78–80.

Drozdov, Y. N., 1984, "Calculating the Wear of a Screw and Nut Transmission with Sliding Friction," *Soviet Engineering Research*, Vol. 4, No. 5, pp. 6–8.

Levit, G. A., 1963a, "Recirculating Ball Screw and Nut Units," *Machines and Tooling*, Vol. XXXIV, No. 4, pp. 3–8.

Levit, G. A., 1963b, "Calculations of Recirculating Ball Screw and Nut Transmissions," *Machines and Tooling*, Vol. XXXIV, No. 5, pp. 9–16.

Lin, M. C., Ravani, B., and Velinsky, S. A., 1994, "Kinematics of the Ball Screw Mechanism," ASME JOURNAL OF MECHANICAL DESIGN, *in press*.

Mukhortov, V. N., 1982, "Increasing the Life of Anti-Friction Screw-and-Nut Transmissions," *Soviet Engineering Research*, Vol. 2, No. 10, pp. 86–87.